

Supporting Information: Ultrasensitivity of water exchange kinetics to the size of metal ion

Yuno Lee,[†] D. Thirumalai,[‡] and Changbong Hyeon^{*,†}

[†]*School of Computational Sciences, Korea Institute for Advanced Study, Seoul 02455, Korea*

[‡]*Department of Chemistry, University of Texas, Austin, TX 78712-1224, United States*

E-mail: hyeoncb@kias.re.kr

Supporting Information

Methods

Tetrahedral order parameter for H-bond network. The extent of H-bond network formed among water molecules is quantified using the local tetrahedral order parameter¹ averaged over position at r from the center of metal ion, which is defined as

$$\langle Q \rangle(r) = \frac{1}{N(r)} \sum_{k=1}^{N(r)} \left\{ 1 - \frac{3}{8} \sum_{i=1}^3 \sum_{j=i+1}^4 \left[\cos \psi_{ikj} + \frac{1}{3} \right]^2 \right\}. \quad (\text{S1})$$

where $N(r)$ is the number of water oxygens present at the interval $(r, r + dr)$, i and j denote the nearest neighbors to the water molecule k , and ψ_{ikj} denote the angle between the water molecules i , k , and j .

Non-bonded interaction between water and ions. Coulombic and Lennard-Jones (LJ) potentials were used to calculate electrostatic and van der Waals (vdW) contributions to non-bonded interaction between water and ions: (1) The electrostatic interaction between two atoms is calculated using Coulombic potential:

$$V_{\text{elec}}(r_{ij}) = k \frac{q_i q_j}{\epsilon_r r_{ij}}, \quad (\text{S2})$$

where the electric conversion factor $k = 1/4\pi\epsilon_0 \approx 138.94 \text{ kJ mol}^{-1} \text{ nm } e^{-2}$, ϵ_r is the relative dielectric constant set to 1, and q_i is the charge of atom i ; (2) The van der Waals (vdW) interaction between two atoms is modeled using the LJ potential

$$V_{LJ}(r_{ij}) = 4\epsilon_{ij} \left[\left(\frac{\sigma_{ij}}{r_{ij}} \right)^{12} - \left(\frac{\sigma_{ij}}{r_{ij}} \right)^6 \right] \quad (\text{S3})$$

where i and j are the indices of two atoms, r_{ij} is the distance between the atoms i and

j . ε_{ij} is the depth of energy minimum and σ_{ij} is the distance at which the interatomic potential becomes zero. In AMBER and CHARMM force fields, the atomic radius σ_i and the strength of vdW interaction ε_i are defined for each atom type; σ_{ij} and ε_{ij} are calculated from $\sigma_{ij} = (\sigma_i + \sigma_j)/2$ and $\varepsilon_{ij} = \sqrt{\varepsilon_i \varepsilon_j}$, respectively. In GROMOS force fields (GROMOS87 and GROMOS96) the LJ potential is expressed as $V_{LJ}(r_{ij}) = C_{ij}^{(12)}/r_{ij}^{12} - C_{ij}^{(6)}/r_{ij}^6$ where $C_{ij}^{(6)} = \sqrt{C_{ii}^{(6)} C_{jj}^{(6)}}$ and $C_{ij}^{(12)} = \sqrt{C_{ii}^{(12)} C_{jj}^{(12)}}$, $C_i^{(6)}$ and $C_i^{(12)}$ are defined for each atom type, and they are related to the LJ parameters in AMBER and CHARMM as $C_i^{(6)} = 4\varepsilon_i \sigma_i^6$ and $C_i^{(12)} = 4\varepsilon_i \sigma_i^{12}$.

Protocols of all-atom MD simulation. We performed MD simulations of water and metal ion (Mg^{2+} , Ca^{2+} , and Na^+) ions using 4 different biomolecular force fields: CHARMM27, AMBER03, GROMOS87, and GROMOS96.² All the MD simulations were performed with GROMACS program (ver. 4.5.4).^{3,4} In the simulation box of $\sim 6.0 \times 7.5 \times 6.8 \text{ nm}^3$ containing 10,000 water molecules with periodic boundary condition, we placed 10 metal ions and neutralized the excess charge with Cl^- ions, which corresponds to $\sim 55 \text{ mM}$ salt concentration in which metal ions are more than 30 \AA apart from each other. Although one might be concerned about a possible effect of high salt concentration ($\sim 55 \text{ mM}$) on the water dynamics, the relaxation kinetics of water from ion is practically identical at ten fold lower ion concentration ($\sim 5.5 \text{ mM}$) in which only a single metal ion is placed in the simulation box (Figure S8).

The electrostatic potential was calculated using Particle Mesh Ewald (PME) method.⁵ At the beginning of each simulation, the total energy of the system was minimized through the steepest descents algorithm until the system reaches a tolerance value of $2,000 \text{ kJ mol}^{-1} \text{ nm}^{-1}$. Position-restrained MD simulations were performed for 100 ps in NVT ensemble at 300 K, followed by 100 ps of equilibration under NPT ($P = 1 \text{ bar}$) ensemble. Production run for each system was generated for 100 ns in the NPT ensemble with V-rescale thermostat⁶ and Parrinello-Rahman barostat.⁷

Radial distribution functions of water around an ion. We used the radial distribution function (RDF)⁸ $g(r)$ to quantify the distribution of water molecules on a metal ion. For a given $g(r)$, the local density of water at distance r from the ion at the origin can be evaluated using $\rho(r) = \rho g(r)$ where $\rho = N/V$ is the average density of water. Thus, water coordination number in the i -th hydration shell can be calculated using $CN_i = 4\pi \int_{r_{i-1,i}^{\min}}^{r_{i-1,i}^{\max}} \rho g(r) r^2 dr$ where $i = 1, 2$. For $i = 1$, $r_{0,1}^{\min} = 0$ and $r_{0,1}^{\max}$ is the position of the local minimum in the RDF between the peaks of 1HS (r_1) and 2HS (r_2). For $i = 2$, $r_{1,2}^{\min} = r_{0,1}^{\max}$ and $r_{max,2}$ is the position of the second local minimum in the RDF (minimum position of RDF between the peaks of 2HS and 3HS) .

Correlation function for hydration kinetics. To obtain the average lifetime (or residence time) of water molecules on metal ions, we first calculate the autocorrelation function of water molecules on metal ions:^{9,10}

$$C(t) = \langle h(0)h(t) \rangle = \frac{1}{T-t} \int_0^{T-t} \frac{1}{N(t')} \sum_{i=1}^{N(t')} h_i(t'+t) h_i(t') dt' \quad (\text{S4})$$

where $h_i(t) = 1$ when the i -th water-ion contact is formed; otherwise, $h_i(t) = 0$. The notation $\langle \dots \rangle$ denotes both the time average along the trajectory and the ensemble average over the water-ion pairs ($i = 1, 2, \dots N(t')$) at time t' . Since $C(t)$ is the survival probability of the ion-water pair at time t , the average water lifetime on metal ion is obtained from $\tau = \int_0^\infty C(t) dt$.

Potential of mean force calculation using umbrella sampling technique. Umbrella sampling with harmonic potential $w_i(x) = (k/2)(r - r_i)^2$ was used to calculate the potential of mean force (PMF) along the reaction coordinate, r , which is defined as the distance between Mg^{2+} and water oxygen ($r \equiv |\vec{r}_{O_w} - \vec{r}_{\text{Mg}^{2+}}|$). The reference distance, r_i , was changed from 1.6 Å to 6 Å with 0.1 Å interval and from 6 Å to 10 Å with 0.5 Å interval. The initial

conformations were obtained from a trajectory generated by pulling water molecule from 1.6 Å to 10 Å with $k = 5 \times 10^3$ kJ/(mol·Å²), and equilibrated with position-restrained MD simulation for 20 ps under NPT ensemble. The production run was simulated for 1 ns with a force constant $k = 650$ kJ/(mol·Å²) for the sampling windows in the range of (1.6 – 6) Å and $k = 50$ kJ/(mol·Å²) for the range of (6 – 10) Å. We obtained the PMF by applying the weighted histogram analysis method (WHAM) to the distance distributions obtained at varying r_i .¹¹

Orientalional relaxation time of water on metal ion. The mean orientational relaxation time (τ_{OR}) of water is evaluated using the autocorrelation function of orientational order parameter, $\langle P_2(t)P_2(0) \rangle$ where $P_2(t) = \frac{1}{2}(3 \cos^2(\delta\theta(t)) - 1)$. $\delta\theta(t) = \theta(t) - \theta(0)$ is the angle between dipole vectors of a water molecule at times t and 0.

Analyses

Effects of ion on H-bond network of bulk water. Insertion of a metal ion in aqueous solution produces a radially symmetric field, which aligns the water molecules towards the ion by locally perturbing the water hydrogen bond (H-bond) network. The average tetrahedral order parameter $\langle Q \rangle(r)$ (Eq.S1, Figure S1),¹ as a function of the radial distance r from the center of metal ions shows the effect of metal ion on the H-bond network formed in the bulk water. The tetrahedral alignment of H-bonds, a quintessential signature of water H-bond network, in bulk quantified using $\langle Q \rangle(r)$ yields $\langle Q \rangle(r \gg 1) \approx 0.49$. Local perturbation due to metal ion on the water H-bond network leads to a decrease of $\langle Q \rangle(r)$ in the metal ion surfaces to $\langle Q \rangle \sim 0.39 - 0.44$, the trend of which is similar for all three metal ions (see the results in Figure S1).

Free energy profiles and water exchange time on Ca^{2+} and Na^+ . The free energy barriers for water unbinding from Ca^{2+} and Na^+ are $\Delta G^\ddagger/k_B T_r = 6.42 - 7.42$ (Ca^{2+}), $3.95 - 4.70$ (Na^+). The water lifetime τ is directly available from the calculation using $C(t)$ (see Equation S4 in Method) on Na^+ and Ca^{2+} (see Table 3), which are $\tau^{\text{H}_2\text{O}/\text{Na}^+} = 21 - 39$ ps and $\tau^{\text{H}_2\text{O}/\text{Ca}^{2+}} = 117 - 753$ ps, thus allowing us to determine the prefactor (τ_o) in the Arrhenius equation $\tau = \tau_o e^{\Delta G^\ddagger/k_B T}$, corresponding to the inverse of the attempt frequency at the bound state in free energy profile. For τ_o , we obtain $\tau_o^{\text{H}_2\text{O}/\text{Na}^+} = 0.31 - 0.41$ ps and $\tau_o^{\text{H}_2\text{O}/\text{Ca}^{2+}} = 0.24 - 0.45$ ps, the values that are only slightly larger than the prefactor of the transition state theory $\tau_o^{\text{TST}} = h/k_B T \approx 0.16$ ps.

Water exchange time using the extrapolation of results from pseudo-magnesium ion (Mg^{z+}) to Mg^{2+} . In order to make a first rough estimate of $\tau^{\text{H}_2\text{O}/\text{Mg}^{2+}}$, the mean

lifetime of water associated with Mg^{2+} , we surmised that the activation barrier for water dissociation is dominated by charge-charge attraction between Mg^{2+} and water oxygen, i.e., $\Delta G^\ddagger \sim z/r_1(\sigma)$, where r_1 is the position of the 1HS of an ion for a given σ . Since a direct simulation of water exchange kinetics is feasible for a pseudo-magnesium ion, Mg^{z+} , with (i) reduced charge (z) and (ii) increased vdW radius (σ) as an alternative, we performed simulations to extrapolate the kinetic results to $z = 2$ and $\sigma = \sigma^*$ where σ^* is the vdW radius of Mg^{2+} used in the force fields (see Table S1). To be specific, we vary z in Mg^{z+} from $z = 1.0, 1.1, 1.2$, to a maximal value at which the corresponding $C(t)$ decays at least below 0.5 so that we can reliably fit $C(t)$ and calculate the mean lifetime using $\tau = \int_0^\infty C(t) dt$. The results of the mean water lifetime on pseudo-magnesium ion with a reduced charge, Mg^{z+} , are extrapolated to $z = 2.0$ (Figure S6a). For $z = 1.1 - 1.5$, our simulation confirms $\log \tau \sim z$ (Figure S6a), and the extrapolated values of τ at $z = 2.0$ are found $\tau \approx 3$ ms for all four force fields we tested (Figure S6a). Next, we simulated the water dynamics on pseudo-magnesium ion by gradually reducing the vdW radius σ from a large value towards the actual size parameter used for Mg^{2+} , σ^* (see Table S1 for the σ^* value for each force

field). The free energy barrier is expected to scale as $\Delta G^\ddagger \propto 1/r_1$. Thus, we used the relationship of $\tau \sim e^{r_1^*/r_1}$ to extrapolate the value of τ at $r_1 = r_1^*$, where r_1^* is the position of the 1HS at $\sigma = \sigma^*$. The estimated value of τ using this size extrapolation method is found in the range of $\tau = 1 - 10$ ms, which is similar to $\tau \approx 3$ ms obtained from the charge extrapolation.

Although the above two extrapolations using z and σ variations provide a consistent result for water lifetime, the value is still an order of magnitude greater than the estimates from the PMF calculation and three orders of magnitude greater than the measured value reported by NMR. Furthermore, the kinetic data obtained from the two methods fail to collapse on a single relationship of $\tau \sim e^{z/r_1}$, displaying two separate branches of data points (Figure S6c), which nullifies our hypothesis that the activation barrier is determined mainly by electrostatic attraction between ion and water. A further analysis was also made by considering the entire contributions from electrostatics and vdW interactions between an ion and a water molecule; however, the data points on the plot made for $\log \tau$ versus $|E_{NB}|$ (Figure S6d) again fail to collapse, implying that the energetic contribution alone cannot account for the water exchange kinetics.

Mapping the hydrodynamic radius (r_1) to vdW radius (σ). We propose the following empirical non-bonded interaction between ion (M^{z+}) and water molecule, consisting of (i) the electrostatic attractive interaction between ion and water oxygen, (ii) the electrostatic repulsive interaction between ion and two water hydrogens, and (iii) Lennard Jones interaction between ion and water oxygen:

$$V(r) = k \frac{z_{M^{z+}} z_{O_W}}{\epsilon_r r_{M^{z+}O_W}} + 2k \frac{z_{M^{z+}} z_{H_W}}{\epsilon_r r_{M^{z+}H_W}} + \epsilon_{M^{z+}O_W} \left[\left(\frac{\sigma_{M^{z+}O_W}}{r} \right)^{12} - \left(\frac{\sigma_{M^{z+}O_W}}{r} \right)^6 \right] \quad (S5)$$

where $\sigma_{M^{z+}O_W} = (\sigma_{M^{z+}} + \sigma_{O_W})/2$ and $\epsilon_{M^{z+}O_W} = (\epsilon_{M^{z+}} \epsilon_{O_W})^{1/2}$ (see Table S1). The most probable location of the 1HS from RDF (r_1^{RDF}) and r_1 value which minimizes this potential

$V'(r)|_{r=r_1} = 0$ agrees with an error $< 1\%$, i.e., $|r_1^{\text{RDF}} - r_1|/r_1 < 0.01$. Therefore, with other parameters ($\varepsilon_{\text{M}^{z+}\text{O}_W}$, z_{O_W} , z_{H_W} , and σ_{O_W}) being fixed and given the desired hydrodynamic radius r_1^* , this empirical potential can be used to obtain the corresponding value of ionic size parameter $\sigma_{\text{M}^{z+}}^*$. Therefore, $r_1^* = 2.04 \text{ \AA}$ for the hydrodynamic radius of Mg^{2+} is mapped to $\sigma_{\text{Mg}^{2+}}^*/\text{\AA} = 2.42$ (CHARMM27), 1.64 (AMBER03), 2.10 (GROMOS96), 2.05 (GROMOS87).

Water dynamics in bulk. The characteristic bent shape of water molecule and its ability to be both H-bond acceptor and donor give rise to an interesting dynamical behavior in the process of H-bond disruption. With quantum mechanical effects being ignored, the auto-correlation function of water H-bond displays fine structure in different time domain as discussed by Luzar and Chandler decades ago.¹² In the time scale associated with the dissociation of water from the 1st shell of water-water H-bond RDF, the H-bond relaxation dynamics of water is well described by $C_{\text{HB}}(t) = 0.459e^{-t/1.12 \text{ ps}} + 0.520e^{-t/3.27 \text{ ps}} + 0.021e^{-t/25.1 \text{ ps}}$, which confers the lifetime of H-bonded water in the first solvation shell $\tau_{\text{HB}} = \int_0^\infty C_{\text{HB}}(\tau)d\tau = 2.7 \text{ ps}$ (Figure S7a). However, there is a fine structure in dynamics at sub-picosecond time scale $t \sim 0.1 \text{ ps}$, which reflects the more detailed dynamics occurring inside the 1st shell of water RDF. The inset in Figure S7a, which displays the average rate of change in H-bond population ($k(t) = -dC(t)/dt$) has a hump at $\sim 0.1 \text{ ps}$; water H-bond can transiently rupture and reform due to rotational motion of water molecules while maintaining the positional correlation between two water oxygens for $\lesssim 3 \text{ ps}$.¹²

Table S1: Parameters for metal ion and water in CHARMM27, AMBER03, GROMOS87, and GROMOS96 force fields.^a

system	z^* (e) ^b	σ^* (Å) ^c	ε (kcal · mol ⁻¹) ^d
MG ^{CHARMM27}	2	2.11	0.015
MG ^{AMBER03}	2	1.41	0.895
MG ^{GROMOS96}	2	1.93	0.075
MG ^{GROMOS87}	2	1.93	0.075
CA ^{CHARMM27}	2	2.44	0.120
CA ^{AMBER03}	2	3.05	0.460
CA ^{GROMOS96}	2	2.81	0.121
CA ^{GROMOS87}	2	2.81	0.121
NA ^{CHARMM27}	1	2.43	0.047
NA ^{AMBER03}	1	3.33	0.003
NA ^{GROMOS96}	1	2.58	0.015
NA ^{GROMOS87}	1	2.58	0.015
CL ^{CHARMM27}	-1	4.04	0.150
CL ^{AMBER03}	-1	4.40	0.100
CL ^{GROMOS96}	-1	4.45	0.107
CL ^{GROMOS87}	-1	4.45	0.106
O _w ^{TIP3P}	-0.834	3.15	0.152
H _w ^{TIP3P}	0.417	0	0
O _w ^{SPC}	-0.82	3.17	0.155
H _w ^{SPC}	0.41	0	0

^a For the CHARMM27 force field, all the ion parameters were adopted from Roux and coworkers' studies.¹³⁻¹⁵ For the AMBER03, AMBER-adapted Åqvist parameters¹⁶ were used for the Mg²⁺ and Ca²⁺, and the parameters for the Na⁺ and Cl⁻ are from Sangster¹⁷ and Dang,¹⁸ respectively. For the two GROMOS96 and 87, all the ion parameters from Berendsen and coworkers.^{19,20}

^b Valence (charge) of ions and atoms (see Eq.S2).

^c van der Waals radii ($2^{1/6} \times \sigma^*$, diameter) of ions and water oxygen (see Eq.S3).

^d Prefactor of Lennard Jones potential (see Eq.S3).

Table S2: Water structure on metal ions and the interaction energy between an ion and a water molecule in the first hydration shell

system	water model	CN ₁ (Å)		CN ₂ (Å)		E_{elec}^a (kcal · mol ⁻¹)	E_{LJ}^b (kcal · mol ⁻¹)
		r_1^*/r_2^* (Å)	($r_{\text{min},1}$, $r_{\text{max},1}$)	($r_{\text{min},2}$, $r_{\text{max},2}$)	($r_{\text{min},2}$, $r_{\text{max},2}$)		
MG ^{CHARMM27}	TIP3P	1.976/4.234	6 (0, 3.0)	14.94 (3.0, 5.10)		-71.76	4.87
MG ^{AMBER03}	TIP3P	1.994/4.223	6 (0, 3.0)	15.23 (3.0, 5.14)		-70.56	4.12
MG ^{GROMOS87}	TIP3P	1.975/4.221	6 (0, 3.0)	14.81 (3.0, 5.08)		-71.91	4.56
MG ^{GROMOS96}	SPC	1.985/4.184	6 (0, 3.0)	13.53 (3.0, 4.98)		-70.77	4.44
CA ^{CHARMM27}	TIP3P	2.286/4.591	6.96 (0, 3.0)	20.18 (3.0, 5.66)		-54.66	4.19
CA ^{AMBER03}	TIP3P	2.705/4.990	8.93 (0, 3.5)	23.55 (3.5, 6.02)		-39.23	3.06
CA ^{GROMOS87}	TIP3P	2.459/4.759	7.99 (0, 3.2)	22.65 (3.2, 5.90)		-47.32	3.68
CA ^{GROMOS96}	SPC	2.469/4.719	7.97 (0, 3.2)	21.48 (3.2, 5.84)		-46.52	3.62
NA ^{CHARMM27}	TIP3P	2.319/4.592	5.72 (0, 3.1)	19.94 (3.1, 5.62)		-25.45	2.09
NA ^{AMBER03}	TIP3P	2.409/4.670	5.77 (0, 3.3)	20.30 (3.3, 5.68)		-23.77	2.39
NA ^{GROMOS87}	TIP3P	2.259/4.547	5.53 (0, 3.0)	21.06 (3.0, 5.70)		-26.93	2.30
NA ^{GROMOS96}	SPC	2.270/4.497	5.48 (0, 3.0)	19.39 (3.0, 5.58)		-26.32	2.25

$$^a E_{\text{elec}} = \frac{1}{N_{\text{H}_2\text{O}}} \frac{1}{N_{\text{Mg}^{2+}}} \sum_{i \in \text{Mg}^{2+}} \sum_{j \in \text{H}_2\text{O}} V_{\text{elec}}(r_{ij}) \Theta(r_{\text{max},1} - r_{ij})$$

$$^b E_{\text{LJ}} = \frac{1}{N_{\text{H}_2\text{O}}} \frac{1}{N_{\text{Mg}^{2+}}} \sum_{i \in \text{Mg}^{2+}} \sum_{j \in \text{H}_2\text{O}} V_{\text{LJ}}(r_{ij}) \Theta(r_{\text{max},1} - r_{ij})$$

Table S3: Mean water lifetimes on metal ions estimated from MD simulations

system	water model	τ_{PMF} (μs) ^a	$\tau^{(1)}$ ($R_c/\text{\AA}$)	$\tau^{(2)}$ (ps) ^c ($R_c/\text{\AA}$)
MG ^{CHARMM27}	TIP3P	582 – 804	1437 μs ^b	16.8 (5.10)
MG ^{AMBER03}	TIP3P	664 – 831	164 μs ^b	17.1 (5.14)
MG ^{GROMOS87}	TIP3P	282 – 373	1649 μs ^b	17.7 (5.08)
MG ^{GROMOS96}	SPC	145 – 174	363 μs ^b	20.8 (4.98)
CA ^{CHARMM27}	TIP3P	-	117 ps (3.0)	18.4 (5.66)
CA ^{AMBER03}	TIP3P	-	255 ps (3.5)	18.9 (6.02)
CA ^{GROMOS87}	TIP3P	-	679 ps (3.2)	18.9 (5.90)
CA ^{GROMOS96}	SPC	-	753 ps (3.2)	23.5 (5.84)
NA ^{CHARMM27}	TIP3P	-	34 ps (3.1)	16.3 (5.62)
NA ^{AMBER03}	TIP3P	-	21 ps (3.3)	16.1 (5.68)
NA ^{GROMOS87}	TIP3P	-	34 ps (3.0)	17.4 (5.70)
NA ^{GROMOS96}	SPC	-	39 ps (3.0)	19.9 (5.58)

^a The τ_{PMF} was calculated using ΔG^\ddagger from PMF of water-Mg²⁺ ($\Delta G^\ddagger/k_B T = 21.53$ (CHARMM27), 21.37 (AMBER03), 20.56 (GROMOS87), 19.71 (GROMOS96)) and the prefactor (τ_o) evaluated in Ca²⁺: 0.24 ps (CHARMM27), 0.32 ps (AMBER03), 0.41 ps (GROMOS87), 0.45 ps (GROMOS96), and those in Na⁺: 0.34 ps (CHARMM27), 0.41 ps (AMBER03), 0.31 ps (GROMOS87), 0.38 ps (GROMOS96). ^b The water lifetime obtained from the universal curve analysis in Figure 3. ^c $\tau^{(2)}$ is the lifetime of water molecules in the second hydration shell.

Table S4: Proportion of associative and dissociative water exchange mechanism for Ca²⁺ and Na⁺ in the four force fields. $\tau_{\text{CN}_1\pm 1}$ is the lifetime of transient intermediate formed via associative (+) or dissociative (-) mechanism.

system	Assoc. (%) / τ_{CN_1+1} (ps)	Dissoc. (%) / τ_{CN_1-1} (ps)	Optimal CN ₁
CA ^{CHARMM27}	88.32 / 2.40	11.68 / 4.05	7
CA ^{AMBER03}	19.04 / 1.25	80.96 / 2.73	9
CA ^{GROMOS96}	46.76 / 1.09	53.24 / 1.94	8
CA ^{GROMOS87}	30.77 / 1.03	69.23 / 2.27	8
NA ^{CHARMM27}	4.45 / 1.00	95.55 / 1.88	6
NA ^{AMBER03}	29.76 / 1.02	70.24 / 1.48	6
NA ^{GROMOS96}	0 / NA	100 / 2.48	6
NA ^{GROMOS87}	0 / NA	100 / 2.72	6

References

- (1) Kumar, P.; Buldyrev, S. V.; Stanley, H. E. *Proc. Natl. Acad. Sci. U. S. A.* **2009**, *106*, 22130–22134.
- (2) Oostenbrink, C.; Villa, A.; Mark, A. E.; Van Gunsteren, W. F. *J. Comput. Chem.* **2004**, *25*, 1656–1676.
- (3) Berendsen, H. J.; van der Spoel, D.; van Drunen, R. *Comp. Phys. Comm.* **1995**, *91*, 43–56.
- (4) Pronk, S.; Páll, S.; Schulz, R.; Larsson, P.; Bjelkmar, P.; Apostolov, R.; Shirts, M. R.; Smith, J. C.; Kasson, P. M.; van der Spoel, D.; Berk, H.; Erik, L. *Bioinformatics* **2013**, *29*, 845–854.
- (5) Darden, T.; York, D.; Pedersen, L. *J. Chem. Phys.* **1993**, *98*, 10089–10092.
- (6) Bussi, G.; Donadio, D.; Parrinello, M. *J. Chem. Phys.* **2007**, *126*, 014101.
- (7) Parrinello, M.; Rahman, A. *J. Appl. Phys.* **1981**, *52*, 7182–7190.
- (8) Allen, M.; Tildesley, D. *Computer simulation of liquids*; Clarendon Press: Oxford, 1987.
- (9) Impey, R.; Madden, P.; McDonald, I. *J. Phys. Chem.* **1983**, *87*, 5071–5083.
- (10) Yoon, J.; Lin, J.-C.; Hyeon, C.; Thirumalai, D. *J. Phys. Chem. B* **2014**, *118*, 7910–7919.
- (11) Kumar, S.; Rosenberg, J. M.; Bouzida, D.; Swendsen, R. H.; Kollman, P. A. *J. Comput. Chem.* **1992**, *13*, 1011–1021.
- (12) Luzar, A.; Chandler, D. *Nature* **1996**, *379*, 55–57.
- (13) Mackerell, A. D.; Banavali, N. K. *J. Comput. Chem.* **2000**, *21*, 105–120.
- (14) Marchand, S.; Roux, B. *Proteins Struct. Funct. Genet.* **1998**, *33*, 265–284.
- (15) Beglov, D.; Roux, B. *J. Chem. Phys.* **1994**, *100*, 9050–9063.
- (16) Aqvist, J. *J. Phys. Chem.* **1990**, *94*, 8021–8024.
- (17) Sangster, M.; Atwood, R. *J. Phys. C* **1978**, *11*, 1541.
- (18) Dang, L. X. *J. Am. Chem. Soc.* **1995**, *117*, 6954–6960.
- (19) Straatsma, T.; Berendsen, H. *J. Chem. Phys.* **1988**, *89*, 5876–5886.
- (20) van Gunsteren, W. F.; Berendsen, H. J. *Biomos, Groningen* **1987**, *24*, 13.

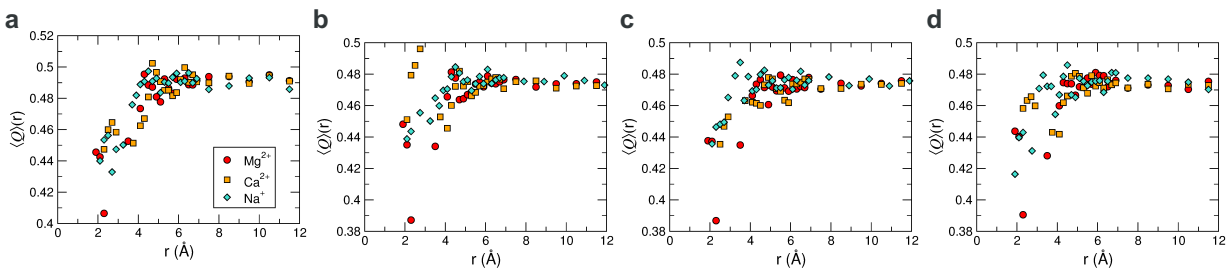


Figure S1: Local tetrahedral order parameter, $Q(r)$, of water molecules as a function of distance from the center of metal ion for (a) GROMOS96, (b) CHARMM27, (c) AMBER03, and (d) GROMOS87 force fields.

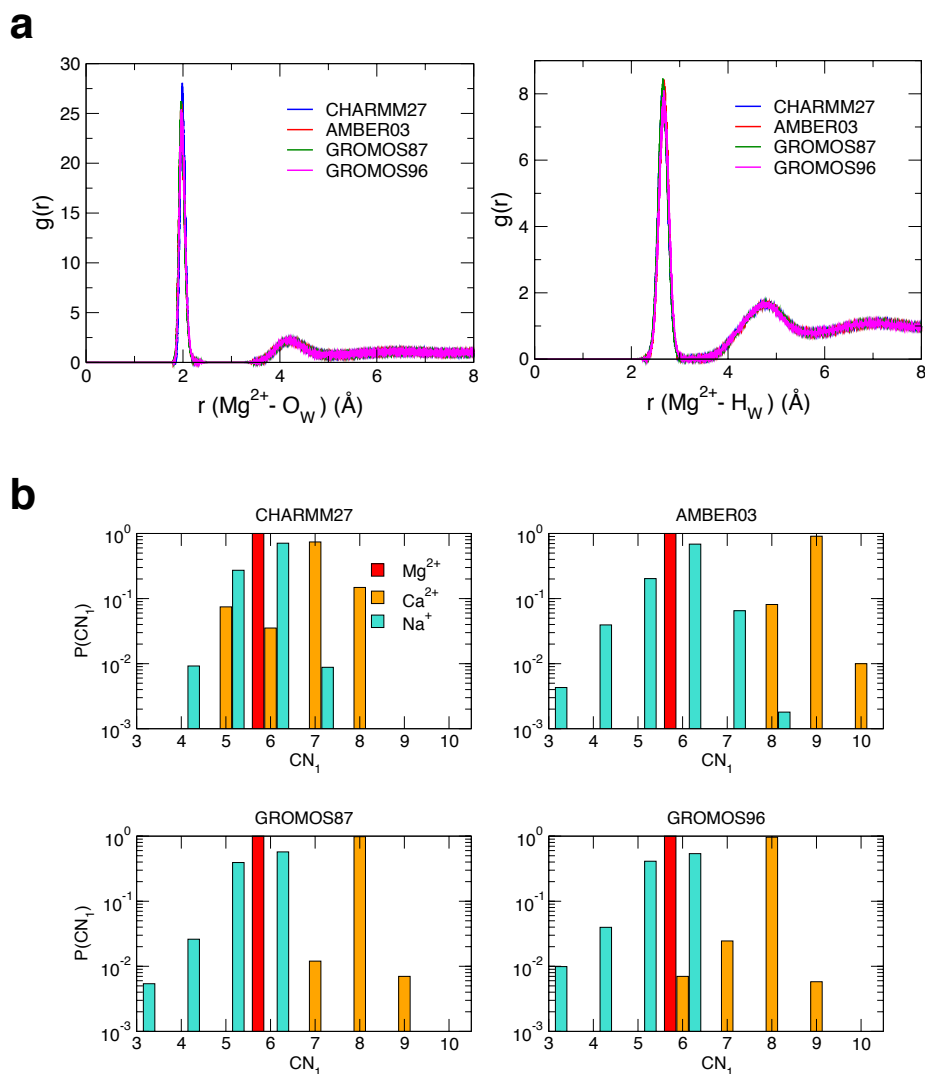


Figure S2: Structure of water molecules around metal ions for the four different force fields. (a) RDF of water oxygen (left) or hydrogen (right) around Mg^{2+} ion from 10 ns simulations using four different force fields. (b) Histogram of the water coordination number in the first hydration shell around Mg^{2+} (red), Ca^{2+} (orange), Na^+ (cyan) for the CHARMM27, AMBER03, GROMOS87, and GROMOS96 force fields.

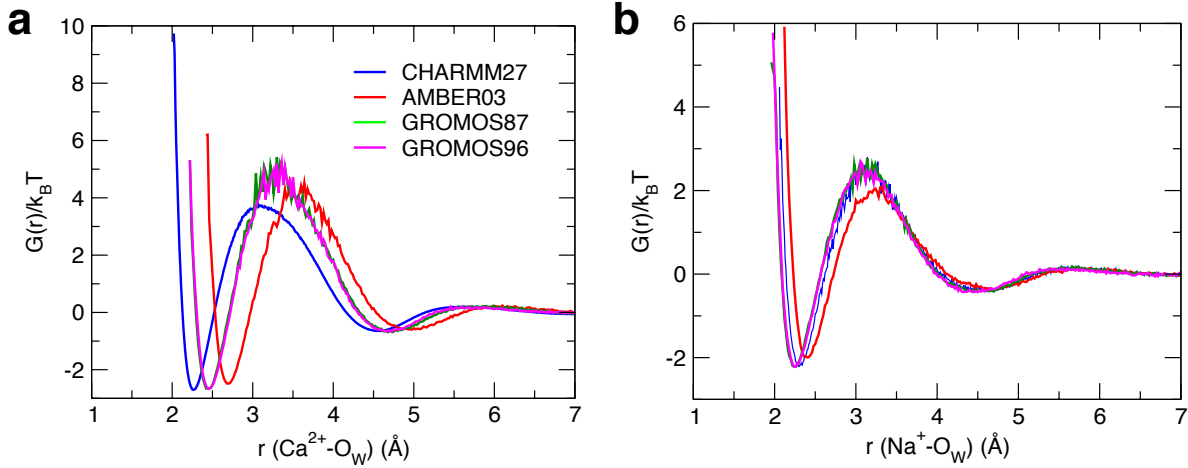


Figure S3: Potential of mean force (PMF) between metal ion and water oxygen obtained from simulations using four different force fields. (a) PMFs, $G(r)$, between Ca^{2+} ion and water oxygen, $G(r) = -k_B T \log g(r)$ where the RDF $g(r)$ was calculated from the 100 ns simulation. The free energy barriers are $\Delta G^\ddagger/k_B T = 6.42$ (CHARMM27), 6.67 (AMBER03), 7.41 (GROMOS87), 7.42 (GROMOS96). (b) PMFs, $G(r)$, between Na^+ ion and water oxygen, $G(r) = -k_B T \log g(r)$ where the RDF $g(r)$ was calculated from the 100 ns simulation. The free energy barriers are $\Delta G^\ddagger/k_B T = 4.62$ (CHARMM27), 3.95 (AMBER03), 4.70 (GROMOS87), 4.63 (GROMOS96).

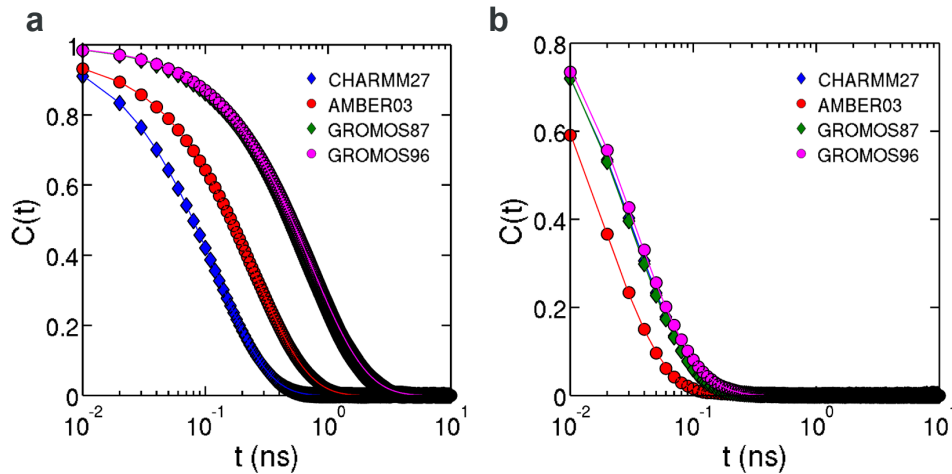


Figure S4: Relaxation kinetics of water on Ca^{2+} and Na^+ ion. The $C(t)$ of (a) Ca^{2+} and (b) Na^+ with four different force fields. Mean water lifetimes of Ca^{2+} ion for the different force fields were estimated as 117 ps (CHARMM27), 255 ps (AMBER03), 679 ps (GROMOS87), 753 ps (GROMOS96). Mean water lifetimes of Na^+ ion for the different force fields were estimated as 34 ps (CHARMM27), 21 ps (AMBER03), 34 ps (GROMOS87), 39 ps (GROMOS96).

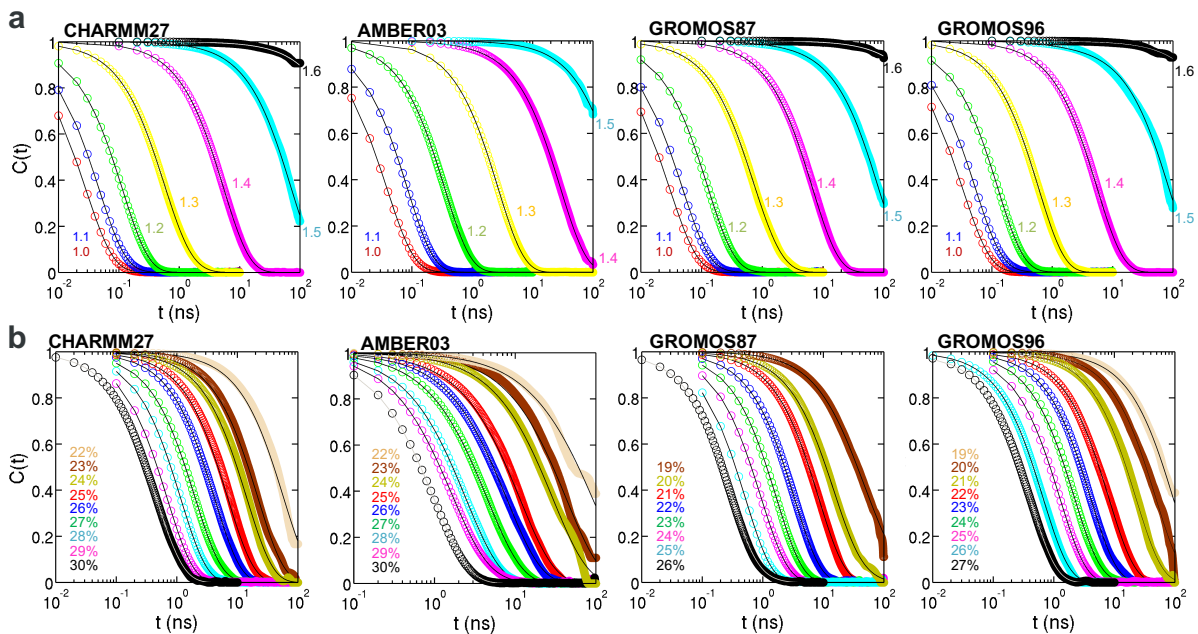


Figure S5: Relaxation kinetics of water from pseudo-magnesium ions for the four different force fields. (a) Time correlation function, $C(t)$, describing the relaxation kinetics of water on pseudo-magnesium ion Mg^{z+} with varying charge z where $z = 1.0, 1.1, 1.2, \dots, 2.0$. (b) $C(t)$ of water on Mg^{2+} with varying size parameter $\sigma_{\text{Mg}^{2+}}$. The size of pseudo-magnesium ($\sigma_{\text{Mg}^{2+}}$), which is greater than that of the original magnesium ion ($\sigma_{\text{Mg}^{2+}}^*$, see Table 1), is provided in percentage $(\sigma_{\text{Mg}^{2+}} - \sigma_{\text{Mg}^{2+}}^*)/\sigma_{\text{Mg}^{2+}}^* \times 100$ (%).

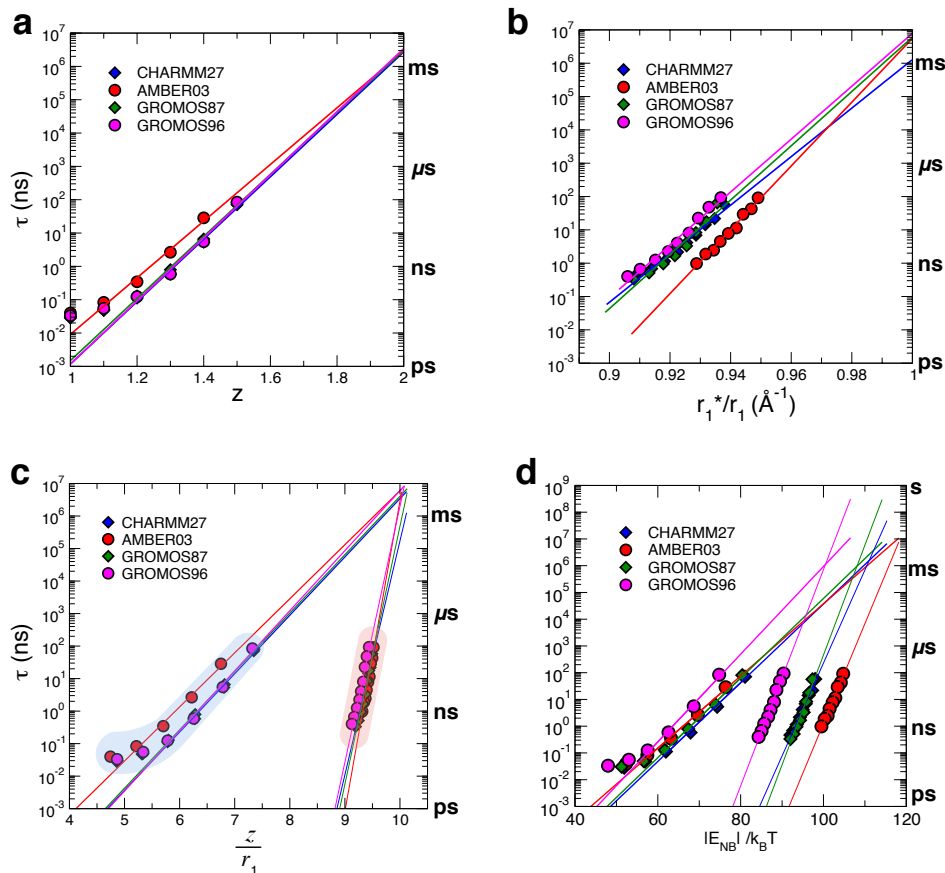


Figure S6: (a) The mean lifetimes (τ) of water around pseudo-magnesium ion obtained from four different force fields as a function of ion charge (z). The extrapolations to $z = 2.0$ gives $\tau = 2 - 3$ ms. (b) τ as a function of the position of 1HS (r_1) which increases with an increasing vdW radius (σ). The data are extrapolated to $r_1^*/r_1 = 1$, which corresponds to the value when $\sigma_{\text{Mg}^{2+}} = \sigma_{\text{Mg}^{2+}}^*$, i.e., when the original size of Mg^{2+} is used. (c) τ as a function of z/r_1 ($[e/\text{nm}]$) that combines the results from (a) and (b). The data points in $4 \leq z/r_1 \leq 7$ (on the blue shade) are obtained by varying the charge, and those in $9 \leq z/r_1 \leq 9.5$ (on the red shade) are obtained by varying the size. (d) Mean water lifetime as a function of total non-bonded interaction energy of a water molecule on an ion calculated by varying the parameters z, r_1 .

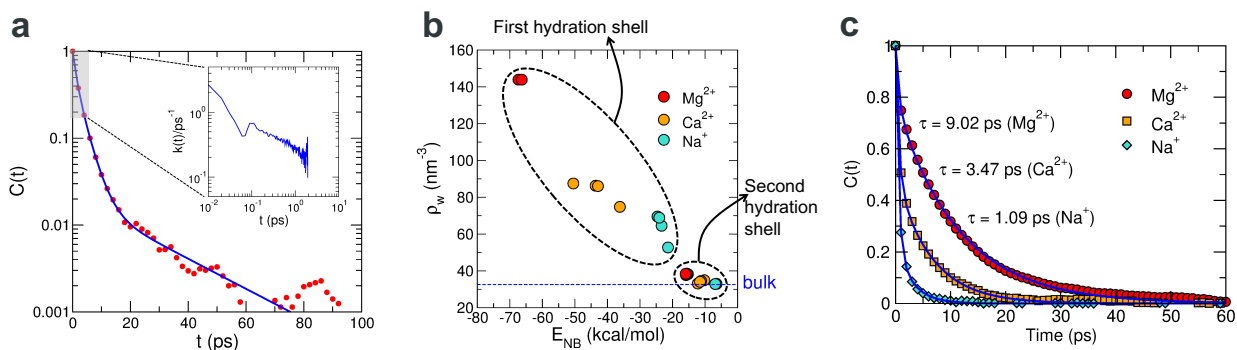


Figure S7: Water dynamics in the bulk and around metal ion. (a) H-bond relaxation dynamics of water in the bulk. (b) Water density (ρ_w) at the first (left) and second hydration shell (right) calculated using the four different force fields as a function of average interaction energy between an ion and water in the corresponding hydration shell. The dashed line at $\rho_w \approx 33 \text{ nm}^{-3}$ is the water density in the bulk. (c) Orientational relaxation dynamics of water molecule on metal ions.

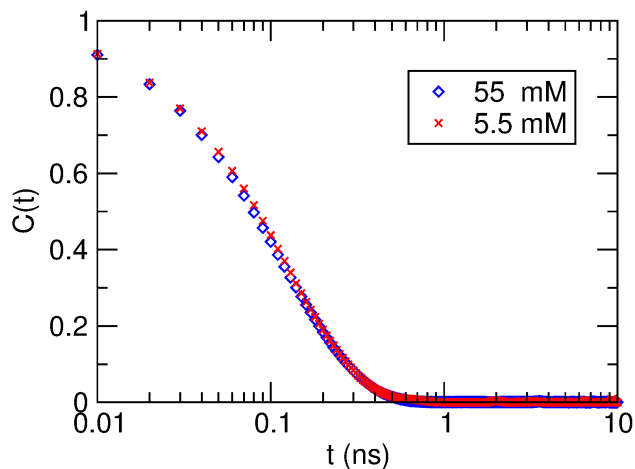


Figure S8: Relaxation kinetics of water from Ca²⁺ at two different ion concentrations, calculated under CHARMM27 force field. The 55 mM result corresponds to the case where 10 Ca²⁺ ions are in the simulation box. Relaxation kinetics of water from Ca²⁺ ion display an almost identical kinetic behavior in the two different concentrations.